

PAPER • OPEN ACCESS

Quantum consensus dynamics by entangling Maxwell demon

To cite this article: Sunguen Ryu *et al* 2022 *New J. Phys.* **24** 033028

View the [article online](#) for updates and enhancements.

You may also like

- [Energy extraction of a chaotic system in a cyclic process: a Szilárd engine perspective](#)
Artur Soriani and Marcus V S Bonança
- [Stochastic thermodynamics for “Maxwell demon” feedbacks](#)
Massimiliano Esposito and Gernot Schaller
- [One-photon atomic cooling with an optical Maxwell demon valve](#)
A Ruschhaupt, J G Muga and M G Raizen



PAPER

Quantum consensus dynamics by entangling Maxwell demon

OPEN ACCESS

RECEIVED

9 November 2021

REVISED

14 February 2022

ACCEPTED FOR PUBLICATION

23 February 2022

PUBLISHED

28 March 2022

Original content from this work may be used under the terms of the [Creative Commons Attribution 4.0 licence](#).

Any further distribution of this work must maintain attribution to the author(s) and the title of the work, journal citation and DOI.



Sungguen Ryu* , Rosa López and Raúl Toral

Instituto de Física Interdisciplinar y Sistemas Complejos IFISC (CSIC-UIB), E-07122 Palma de Mallorca, Spain

* Author to whom any correspondence should be addressed.

E-mail: sungguen@ifisc.uib-csic.es, rosa.lopez-gonzalo@uib.es and raul@ifisc.uib-csic.es**Keywords:** quantum thermodynamics, quantum feedback control, Maxwell demon

Abstract

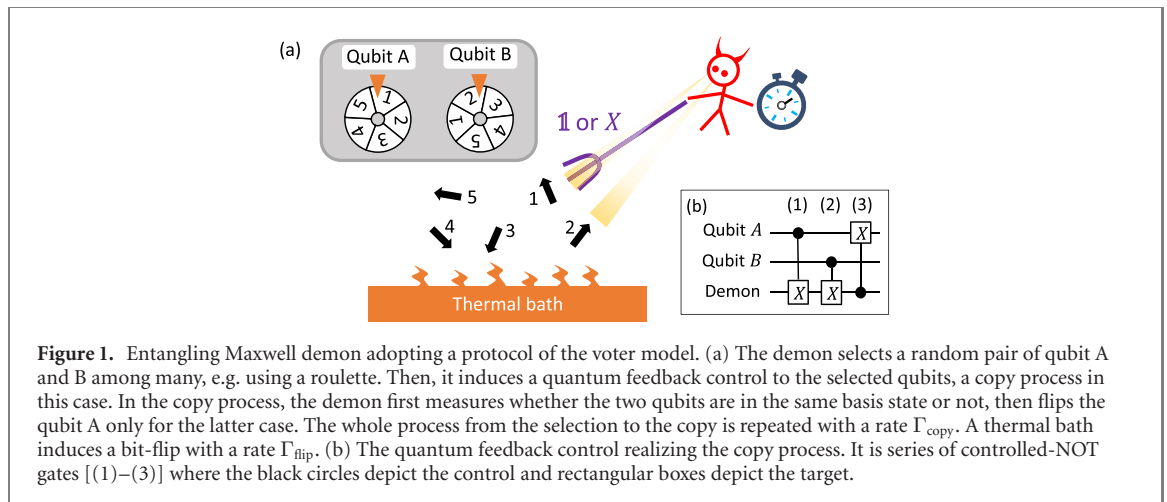
We introduce a Maxwell demon which generates many-body entanglement robustly against bit-flip noises, allowing us to obtain quantum advantage. Adopting the protocol of the voter model used for opinion dynamics approaching consensus, the demon randomly selects a qubit pair and performs a quantum feedback control, in continuous repetitions. We derive upper bounds for the entropy reduction and the work extraction rates by the demon's operation. These bounds are determined by a competition between the quantum–classical mutual information acquired by the demon and the absolute irreversibility of the feedback control. Our finding of the upper bounds corresponds to a reformulation of the second law of thermodynamics under a class of Maxwell demon which generates many-body entanglement in a working substance. This suggests that a general condition for the operation of a successful entangling demon, one for which many-body entanglement stabilization and work extraction are possible, is that the information gain is larger than the absolute irreversibility.

1. Introduction

A modern view of a Maxwell demon is based on a closed-loop feedback control in which the dynamics of a system uses outputs of a measurement as inputs in a smart manner. Within the framework of nanoscale machines, quantum feedback controls involve systematic measurements and manipulations of quantum systems with the aim of extracting useful work or cooling a system [13, 17–19, 22, 31]. The field of thermodynamics of information [13, 29, 33, 36] has clarified the fundamental bounds on entropy reduction and work extraction in terms of quantities such as the quantum–classical mutual information and absolute irreversibility [13]. However, the thermodynamics of continuous quantum feedback [33] remains a largely unexplored issue. Recently, variants of the original Maxwell demon which operate continuously in time have been demonstrated [23, 35], showing an enhancement of the work extraction beyond the conventional feedback control with a limitation given by modified second-law-like inequalities.

Stepping further along this direction, we propose in this paper a new type of Maxwell demon, namely a continuous quantum feedback control, that is capable of generating many-body entanglement in the working substance. Our demon (see figure 1) acts by randomly selecting two qubits A and B among many, and inducing a quantum feedback control on them which reduces entropy and enhances correlation simultaneously. The demon continuously repeats the selection and the feedback control.

In fact, such protocol realizes the quantum steady-state engineering [6, 12, 21, 25, 34, 39–42, 45, 47] as studied in quantum information and optics. The two-qubit quantum feedback control realizes the two-particle dissipations [8, 40–42, 44] whereby one particle's dissipation depends on the state of the other. Previous studies have identified possible types of entangled states which are stabilizable. However, the quantum dynamics, i.e. how entanglement, coherence, and von Neumann entropy evolve in time, still lacks understanding. The mechanism behind the quantum dynamics is nontrivial due to two simultaneous tasks, the random selection and the continuous quantum measurement [2, 10]. Moreover, the fundamental bound of entropy reduction rate by the two-particle dissipations has not been studied before, and an identification of the bound requires a viewpoint from thermodynamics of information.



In this paper, we study the quantum dynamics and the second law of thermodynamics under the action of the entangling Maxwell demon. We first propose a quantum version of the voter model, an entangling Maxwell demon adopting a protocol inspired by the noisy voter model [3, 7, 15, 16, 32], and motivated by the fact that the classical model generates classical correlation of human opinions among agents. Our first main finding is that Greenberger–Horne–Zeilinger (GHZ) entanglement [14, 20, 24] is generated among the working substance and stabilized against the bit-flip noises [5, 9, 43]. During the entanglement generation, the purity and the entropy of the working substance change non-monotonically in time, which turns out to be due to the competition between the information gain and the absolute irreversibility of the feedback control.

Then, as our second main finding, we reformulate the second law of thermodynamics under the action of a generic class of entangling Maxwell demons. We derive an upper bound for the entropy reduction or, equivalently, an upper bound for the work extraction. The bounds are determined by the competition between the quantum–classical mutual information acquired by the demon and the associated absolute irreversibility of the control. We recall that the absolute irreversibility, defined as the sum of the probabilities of the backward trajectories which do not have a corresponding forward trajectory, is responsible, for instance, of the breakdown of the Jarzynski equality in the free gas expansion [26, 27]. In our case, the absolute irreversibility is generally non zero as the quantum measurement in the action of the entangling Maxwell demon projects the state of the working substance to a local subspace which depends on the selection, an inevitable factor hindering the entanglement generation or work extraction. Our findings provide a necessary condition, namely that the information gain should be larger than the absolute irreversibility, to determine when an entangling Maxwell demon can successfully stabilize the many-body entanglement or extract work through the entangled working substance.

This paper is structured as follows. In section 2.1 we present the details of the quantum voter model and the master equation in the Lindblad form. In section 2.2 we present the results of the quantum dynamics and discuss a possible method for the experimental realization. In section 3.1, we derive the upper bounds of the entropy reduction and the work extraction rates by the entangling Maxwell demon. In section 3.2 we give an interpretation of the absolute irreversibility which appears in the bounds. In section 3.3 we show that the non-monotonic behavior in the purity and the entropy of the quantum voter model is due to the competition of the absolute irreversibility and the information gain of the feedback control. In section 3.4, an example of the work extraction by the entangling Maxwell demon is shown. Finally, in section 4 we summarize our main results.

2. Quantum voter model

2.1. Model

In the following, we explain the quantum version of the voter model. Let us consider a system of N qubits ($N \geq 2$). In our analogy, the two level state $|s_i\rangle$ ($|0\rangle$ or $|1\rangle$) of qubit $i = 1, \dots, N$, plays the role of the opinion variable $s_i = 0, 1$ held by an agent of the classical voter model, see figure 1(a). A quantum feedback control (see below) realizes the copy process $C_{i \leftarrow j}$ whereby qubit i copies the state of qubit j . We focus on the case of all-to-all connectivity, so that a copy process $C_{i \leftarrow j}$ of randomly chosen i and $j \neq i$ is induced with rate Γ_{copy} . (See appendix A for comparison with one-dimensional nearest-neighbor connections.) A thermal bath around the system induces bit-flip noise, and the state $|s_i\rangle$ of the qubit i flips ($|0\rangle \rightarrow |1\rangle$ or $|1\rangle \rightarrow |0\rangle$)

with a rate Γ_{flip} for random i . Such flip process corresponds to the transversal noise [5, 9, 43] induced by the dephasing in the basis of $|0\rangle \pm |1\rangle$. Note that, as discussed in section 3.4, Γ_{flip} is determined by the temperature of the bath [38]. When there is no coherence, our system corresponds to the voter model when $\Gamma_{\text{flip}} = 0$ and to the noisy voter model when $\Gamma_{\text{flip}} > 0$ [32].

The copy process $\mathcal{C}_{i \leftarrow j}$ cannot be realized only by unitary dynamics among the N qubits because of the redundancy of the outcomes, e.g. $(s_i, s_j) = (0, 0)$ and $(1, 0)$ both become $(0, 0)$ after the copy process. This process $\mathcal{C}_{i \leftarrow j}$ can be realized instead using a quantum feedback control with an ancilla qubit (which plays the role of a Maxwell demon) effectively measuring whether $s_i = s_j$ or not, see figure 1(b). The joint state of qubits i, j (denoted by Qubit A and B in figure 1), and ancilla, $|s_i s_j s_a\rangle$, changes by the three controlled-NOT (C-NOT) gates as

$$\begin{aligned} |000\rangle &\xrightarrow{(1)} |000\rangle \xrightarrow{(2)} |000\rangle \xrightarrow{(3)} |000\rangle \\ |010\rangle &\rightarrow |010\rangle \rightarrow |011\rangle \rightarrow |111\rangle \\ |100\rangle &\rightarrow |101\rangle \rightarrow |101\rangle \rightarrow |001\rangle \\ |110\rangle &\rightarrow |111\rangle \rightarrow |110\rangle \rightarrow |110\rangle \end{aligned} \quad (1)$$

The first two gates, steps (1) and (2), effectively measure whether $s_i = s_j$ by flipping the ancilla qubit $s_a = 0$ to $s_a = 1$ only when $s_i \neq s_j$, while the third gate, step (3), realizes the copy process. Note that this copy process is not prohibited by the no-cloning theorem [28] because it does not copy an arbitrary state. The ancilla state should be initialized to $s_a = 0$ before starting the copy process, otherwise we obtain the opposite result, i.e. $s_i \neq s_j$ after the feedback. We assume an ideal ancilla in this study, which can be realized by attaching a separate bath [19] that relaxes the ancilla into the state $|0\rangle$ in a time scale much faster than $\Gamma_{\text{copy}}^{-1}$. Below, we focus on the dynamics of the N qubits, tracing out the ancilla.

The copy process $\mathcal{C}_{i \leftarrow j}$ changes the density matrix ρ of the N -qubit state to $\mathcal{C}_{i \leftarrow j}(\rho)$,

$$\mathcal{C}_{i \leftarrow j}(\rho) = \sum_{k=0,1} U_k^{(i)} M_k^{(ij)} \rho M_k^{(ij)\dagger} U_k^{(i)\dagger}. \quad (2)$$

Here, $M_0^{(ij)}$ (resp. $M_1^{(ij)}$) is the measurement operator for the outcome $s_i = s_j$ (resp. $s_i \neq s_j$),

$$M_0^{(ij)} \equiv |0_i 0_j\rangle\langle 0_i 0_j| + |1_i 1_j\rangle\langle 1_i 1_j|, \quad (3)$$

$$M_1^{(ij)} \equiv |0_i 1_j\rangle\langle 0_i 1_j| + |1_i 0_j\rangle\langle 1_i 0_j|. \quad (4)$$

The probability of each one of these outcomes is

$$p_k^{(ij)} = \text{Tr}(M_k^{(ij)} \rho M_k^{(ij)}), \quad \text{for } k = 0, 1. \quad (5)$$

The post-measurement state is

$$\rho_k^{(ij)} \equiv \frac{1}{p_k^{(ij)}} M_k^{(ij)} \rho M_k^{(ij)}. \quad (6)$$

$U_k^{(i)}$ is the feedback operation for each measurement outcome,

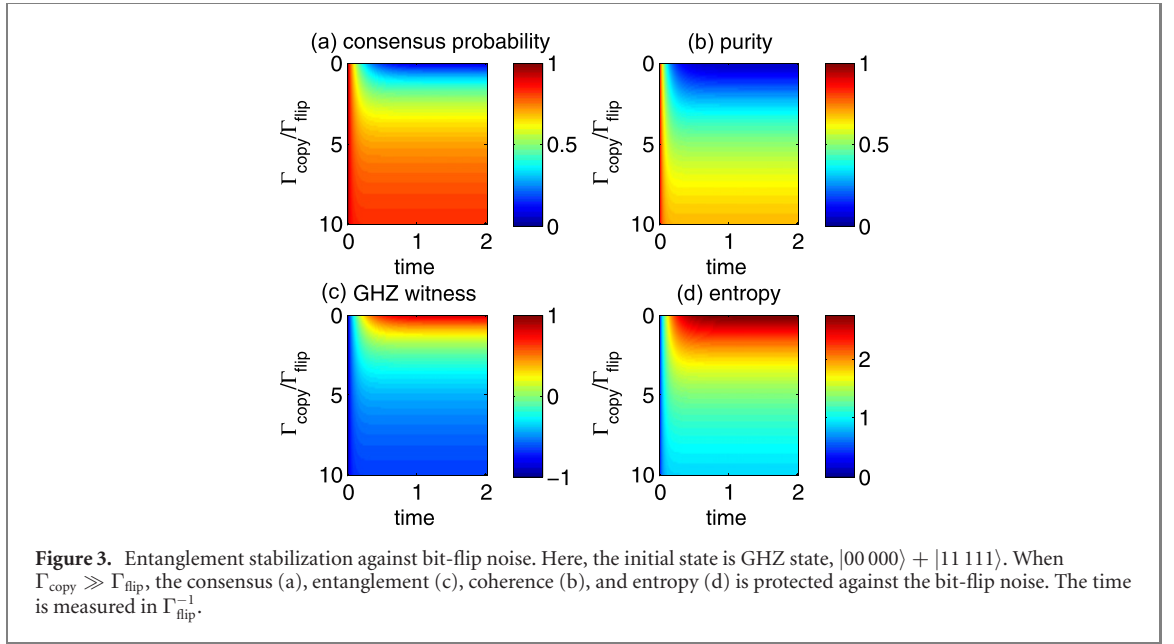
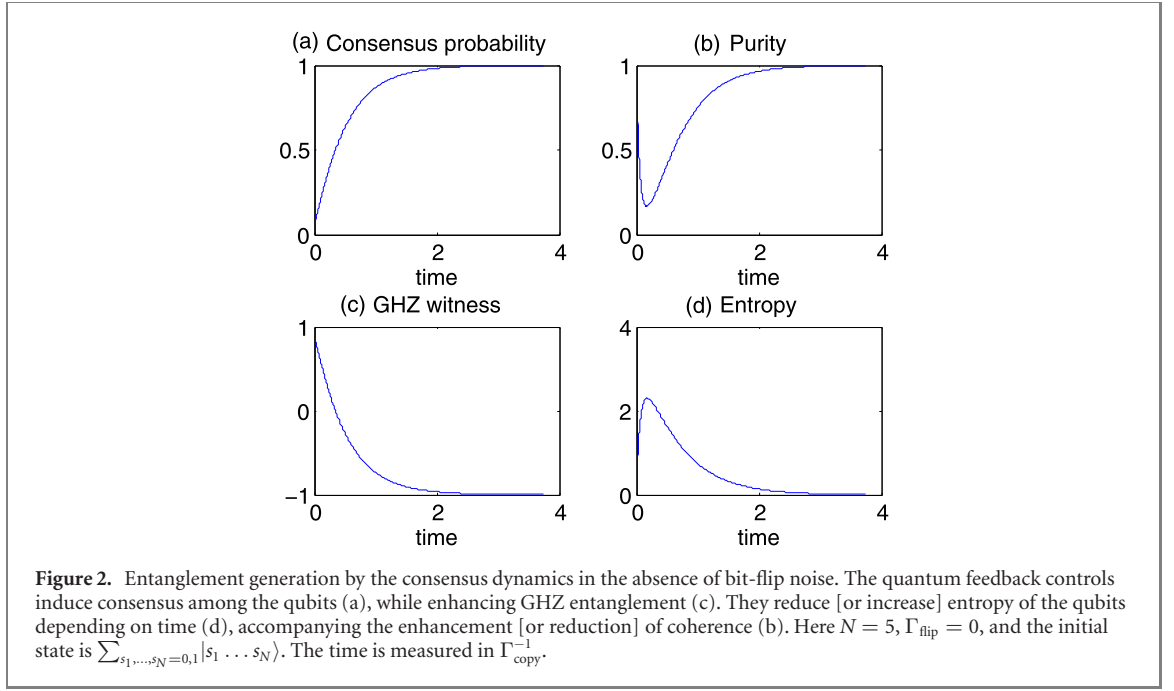
$$U_0^{(i)} = 1, \quad U_1^{(i)} = X_i, \quad (7)$$

where X_i is the operator flipping the state of the qubit i : $X_i|0_i\rangle = |1_i\rangle$ and $X_i|1_i\rangle = |0_i\rangle$. Note that $U_k^{(i)}$ is a unitary and Hermitian operator for the copy process.

The time evolution of ρ by the combined effect of the random copy processes and flips is given by

$$\dot{\rho} = \Gamma_{\text{copy}} \sum_{\substack{i,j=1 \\ i \neq j}}^N (\mathcal{C}_{i \leftarrow j}(\rho) - \rho) + \Gamma_{\text{flip}} \sum_{i=1}^N (X_i \rho X_i - \rho). \quad (8)$$

Equation (8) is derived by considering a completely positive map of a small-time evolution, hence it is in the Lindblad form [38, 45]; see appendix B for details. To obtain the results of figures 2–4 described below, the time evolution of ρ has been calculated by a numerical integration of equation (8). For brevity in the notation, we define the total number of copy processes $\mathcal{C}_{i \leftarrow j}$ for different choices of i and j , as $N_{\text{copy}} \equiv N(N-1)$.



2.2. Entanglement generation and stabilization

To understand the effect generated by the copy process dynamics, we first focus on the case when there is no bit-flip noise, $\Gamma_{\text{flip}} = 0$, a purely consensus dynamics in the language of the voter model [3].

Using as an initial state a symmetric superposition of all possible opinion configurations,

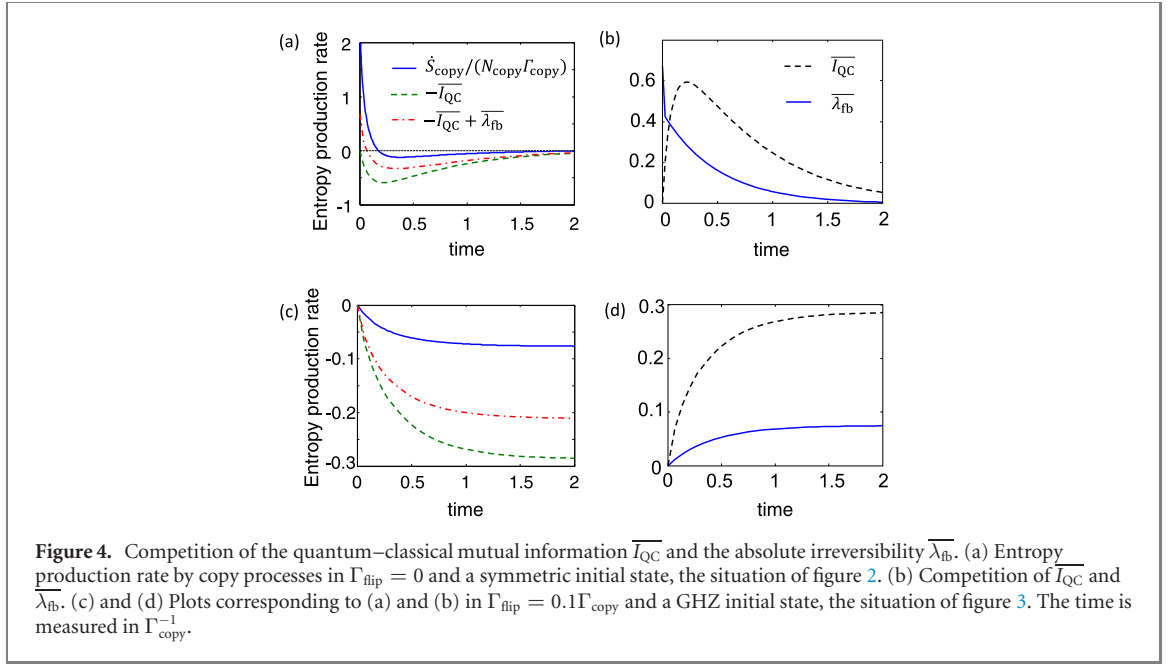
$$|\psi\rangle = \sum_{s_1, \dots, s_N=0,1} |s_1 \dots s_N\rangle, \quad (9)$$

(here and henceforth we omit the normalization factor of all the pure states), the different panels of figure 2 provide evidence that this dynamics generates GHZ entanglement. Panel (a) shows that the consensus probability

$$P_c(\rho) \equiv \langle 0, \dots, 0 | \rho | 0, \dots, 0 \rangle + \langle 1, \dots, 1 | \rho | 1, \dots, 1 \rangle, \quad (10)$$

increases in time and converges to 1. When approaching the consensus, the state tends to the GHZ state, $|0 \dots 0\rangle + |1 \dots 1\rangle$, as evidenced by the GHZ-witness value, defined as [24],

$$W_{\text{GHZ}}(\rho) = 1 - P_c(\rho) - 2|\langle 0, \dots, 0 | \rho | 1, \dots, 1 \rangle|, \quad (11)$$



displayed in panel (c). The negative value of W_{GHZ} means that the state displays a GHZ entanglement, where the lower bound -1 is achieved for the GHZ state [20]. Interestingly, as displayed in panel (d), the von Neumann entropy,

$$S(\rho) = -\text{Tr}(\rho \log \rho), \quad (12)$$

initially increases and then decreases. Of course the coherence, measured by the so-called purity $\text{Tr}(\rho^2)$, also follows the corresponding trend, see panel (b). As discussed in section 3.3, this turns out to be the result of a competition between the quantum–classical mutual information and the absolute irreversibility.

Figure 3 shows that the quantum feedback controls protect the GHZ entanglement against the bit-flip noise. The initial state is now chosen as the five-qubit GHZ state, $|00000\rangle + |11111\rangle$. (See appendix C for the case of an initial state equal to the symmetric superposition). When $\Gamma_{\text{copy}} = 0$ the noise destroys, in time, the consensus, the coherence, and the entanglement, while increasing the entropy. When $\Gamma_{\text{copy}} > 0$, the effect of the noise is reduced, and the different quantities reach a new stationary value. When $\Gamma_{\text{copy}} \gg \Gamma_{\text{flip}}$, the stationary value of the entanglement is significantly large ($W_{\text{GHZ}} < -0.5$ for $\Gamma_{\text{copy}}/\Gamma_{\text{flip}} > 5$).

We now give an example of a three qubits case, for an insight of the GHZ stabilization. Let us consider a GHZ state ρ_{GHZ} which suffered a bit flip with probability ϵ , $(1 - \epsilon)\rho_{\text{GHZ}} + \epsilon\rho_{\text{FGHZ}}$. Here $\rho_{\text{FGHZ}} = \sum_{i=1,2,3} X_i \rho_{\text{GHZ}} X_i / 3$. Then, the copy process recovers the flipped state to GHZ state with probability $1/3$; e.g. for the state where qubit 1 is flipped, among six possible copy processes only $C_{1\leftarrow 2}$ and $C_{1\leftarrow 3}$ return the flipped state to the GHZ state. Thus the copy processes contribute to $\dot{\rho}$ by an amount of $\Gamma_{\text{copy}}\epsilon(\rho_{\text{GHZ}} - \rho_{\text{FGHZ}})/3$. The noise converts the GHZ state to the flipped state or the flipped state to the double flipped state. The double flipped state is the same as the GHZ state with probability of $1/3$, or equal to the single-flipped state otherwise. Thus the noise contributes to $\dot{\rho}$ by amount of $(1 - \epsilon)\Gamma_{\text{flip}}(\rho_{\text{FGHZ}} - \rho_{\text{GHZ}}) + \epsilon\Gamma_{\text{flip}}[(1/3)\rho_{\text{GHZ}} + (2/3)\rho_{\text{FGHZ}} - \rho_{\text{FGHZ}}]$. A steady state is formed at $\epsilon = 3/(4 + \Gamma_{\text{copy}}/\Gamma_{\text{flip}})$, satisfying $\dot{\rho} = 0$ when summing both contributions.

We briefly discuss experimental feasibility. As described in appendix D in detail, the initial state of the symmetric superposition $\sum_{s_1, \dots, s_N=0,1} |s_1 \dots s_N\rangle = (|0\rangle + |1\rangle)^{\otimes N}$ can be prepared when realizing the qubit states 0 and 1 by the $1/2$ -spin up and down state in the z direction, and aligning the spins in the x direction within some error. The repeated random selection of qubit pairs can be realized e.g. using a random number generator. The regime of the fast copy processes, $\Gamma_{\text{copy}} > \Gamma_{\text{flip}}$, can be reached in the experiments like reference [46], as $\Gamma_{\text{copy}} \sim 5$ MHz (according to an operation time ~ 200 ns of a C-NOT gate) and $\Gamma_{\text{flip}} \sim 0.1$ MHz (according to a spin decoherence time of $10 \mu\text{s}$). The regime of the fast ancilla relaxation can also be realized. The relaxation rate of the ancilla is $(D/2)(\Delta E_{\text{anc}}/h) \text{csch}(\Delta E_{\text{anc}}/(kT_{\text{anc}}))$ [19], (k is Boltzmann's constant) when the ancilla of level splitting ΔE_{anc} is coupled to a thermal reservoir of temperature T_{anc} with tunneling probability of D . This value can be as high as GHz scale in typical experimental situations, hence exceeding the rate of copy process Γ_{copy} ; for example, when $T_{\text{anc}} = 0.2$ K, $D = 1$, and $\Delta E_{\text{anc}}/h = 2kT_{\text{anc}}/h \approx 8$ GHz.

We remark a nontrivial aspect of the copy process $C_{i\leftarrow j}$. Generally, the interaction of the qubits with the ancilla leads to the decoherence of the qubits due to the entanglement generation between the qubits and the ancilla. However, the copy process circumvents the destruction of coherence because the ancilla measures only the parity of two qubits. We observe that when the ancilla measures all the information of the two qubits, there is no feature of entanglement generation as in the above result, see appendix E.

3. Second law of thermodynamics

3.1. Upper bounds of entropy reduction and work extraction rate

Here we derive the upper bound of the entropy reduction and work extraction rate by a generic class of entangling Maxwell demons. Our derivations for the bounds are based on the approach of references [13, 33].

We consider a situation in which the working substance, composed of N qubits, is subject to an arbitrary Hamiltonian, arbitrary Markovian dissipations induced by weak coupling to a bath of temperature T , and to the action of the entangling Maxwell demon. In the derivation below we use the specific notation of the quantum voter model, but this can be generalized straightforwardly to a generic entangling Maxwell demon.

We first derive the Lindbladian master equation describing the time evolution of the quantum state of the working substance (which will be called ‘system’ below). Let \mathcal{L}_0 be the Liouvillian in the absence of feedback controls. We consider a time step Δt which is smaller than the repetition period of the selection and feedback, $\Gamma_{\text{copy}}^{-1}$, and the time scales of \mathcal{L}_0 , but larger than the operation time of a single quantum feedback control, e.g. the time for completing the three controlled-NOT gates in the case of the quantum voter model. Then, we obtain the density matrix of the system evolved by both \mathcal{L}_0 and the feedback controls,

$$\rho(t + \Delta t) = \Gamma_{\text{copy}} \Delta t \sum_{i \neq j} C_{i\leftarrow j}(\rho) + (1 - N_{\text{copy}} \Gamma_{\text{copy}} \Delta t) e^{\mathcal{L}_0 \Delta t} \rho + \mathcal{O}(\Delta t^2). \quad (13)$$

Hence, we obtain the master equation,

$$\dot{\rho} = -\frac{i}{\hbar} [H, \rho] + D_{\text{bath}}[\rho] + D_{\text{copy}}[\rho]. \quad (14)$$

Here H is the system Hamiltonian, D_{bath} (resp. D_{copy}) is a Lindblad super-operator describing the dissipation of the system induced by its coupling to the bath (resp. multi-particle dissipations due to the feedback control). In the case of the quantum voter model, D_{copy} is

$$D_{\text{copy}}[\rho] = \Gamma_{\text{copy}} \sum_{i \neq j} [C_{i\leftarrow j}(\rho) - \rho]. \quad (15)$$

As the dissipations by the bath and the feedback control contribute additively to the master equation, the rate of change of system entropy, \dot{S} , is the sum of the two contributions. Using $\dot{S} = -\text{Tr}(\dot{\rho} \ln \rho)$, we obtain

$$\dot{S} = \dot{S}_{\text{bath}} + \dot{S}_{\text{copy}}, \quad (16)$$

$$\dot{S}_{\text{bath}} \equiv -\text{Tr}(D_{\text{bath}}[\rho] \ln \rho), \quad (17)$$

$$\dot{S}_{\text{copy}} \equiv -\text{Tr}(D_{\text{copy}}[\rho] \ln \rho). \quad (18)$$

Note that \dot{S}_{bath} (resp. \dot{S}_{copy}) at time t equals the rate of change of the system entropy assuming that the system $\rho(t)$ is subject only to the dissipation by the bath (resp. feedback controls).

The entropy change rate by the bath is lower-bounded depending on the rate of heat absorption \dot{Q} from the bath as [33],

$$k \dot{S}_{\text{bath}} \geq \dot{Q}/T. \quad (19)$$

On the other hand, the entropy reduction rate by the entangling Maxwell demon, $-\dot{S}_{\text{copy}}$, is upper-bounded as

$$\dot{S}_{\text{copy}} \geq -N_{\text{copy}} \Gamma_{\text{copy}} (\overline{I_{\text{QC}}} - \overline{\lambda_{\text{fb}}}), \quad (20)$$

(see appendix F for its derivation). This is our first main result of this section.

The upper-bound of the entropy reduction rate, equation (20), is determined by the competition of two quantities. First, $\overline{I_{\text{QC}}}$ is the quantum–classical mutual information gained in the feedback control averaged for all the possible selections,

$$\overline{I_{\text{QC}}} \equiv N_{\text{copy}}^{-1} \sum_{i \neq j} I_{\text{QC}}^{(ij)}, \quad (21)$$

$$I_{\text{QC}}^{(ij)} = S(\rho) - \sum_{k=0,1} p_k^{(ij)} S(\rho_k^{(ij)}), \quad (22)$$

where $I_{\text{QC}}^{(ij)}$ is the mutual information given that the qubits i and j are selected. Second, $\overline{\lambda_{\text{fb}}}$ is the absolute irreversibility of a stochastic feedback control (applied to a random pair of qubits), see section 3.2.

Using equations (19) and (20), we obtain

$$k\dot{S} \geq \frac{\dot{Q}}{T} + kN_{\text{copy}}\Gamma_{\text{copy}}(-\overline{I_{\text{QC}}} + \overline{\lambda_{\text{fb}}}). \quad (23)$$

Replacing $\dot{Q} = \dot{E} - \dot{W}$, as given by the first law of thermodynamics (\dot{E} is energy change rate of the system), into equation (23), we obtain the upper bound of the work extraction rate $-\dot{W}$,

$$\dot{W} - \dot{F} \geq kTN_{\text{copy}}\Gamma_{\text{copy}}(-\overline{I_{\text{QC}}} + \overline{\lambda_{\text{fb}}}). \quad (24)$$

This is our second main result of this section. $\dot{F} = \dot{E} - kT\dot{S}$ is the rate of change of nonequilibrium free energy [29].

3.2. Absolute irreversibility

Here we show that the absolute irreversibility $\overline{\lambda_{\text{fb}}}$ of a stochastic feedback control is related to how much the feedback-operated states are different for distinct selections.

As we mentioned earlier, the absolute irreversibility is defined as the sum of probabilities of the backward trajectories which do not have a corresponding forward trajectory [13]. Let ρ be the initial state of the forward trajectory. The final state of the forward trajectory is the result of a stochastic feedback control without knowing which particles were selected,

$$C(\rho) \equiv \frac{1}{N_{\text{copy}}} \sum_{i \neq j} C_{i \leftarrow j}(\rho). \quad (25)$$

This final state becomes the initial state of the backward trajectory, $\rho_r = C(\rho)$, the reference state in the language of the fluctuation theorem (see appendix F).

The absolute irreversibility $\overline{\lambda_{\text{fb}}}$ of a stochastic feedback control is the average of the absolute irreversibility given that it is known which particles were selected,

$$\overline{\lambda_{\text{fb}}} = \frac{1}{N_{\text{copy}}} \sum_{i \neq j} \lambda_{\text{fb}}^{(ij)}, \quad (26)$$

$$\lambda_{\text{fb}}^{(ij)} \equiv \sum_{k=0,1} p_k^{(ij)} \text{Tr}[\Pi_{\text{null}(\rho_k^{(ij)})} U_k^{(i)\dagger} \rho_r U_k^{(i)}]. \quad (27)$$

$\lambda_{\text{fb}}^{(ij)}$ is the absolute irreversibility given that the selected particles were i and j , and $\Pi_{\text{null}(\rho_k^{(ij)})}$ is the projection operator onto the null space of the post-measurement state $\rho_k^{(ij)}$. Using equations (25)–(27) and the relation

$$U_k^{(i)} \Pi_{\text{null}(\rho_k^{(ij)})} U_k^{(i)\dagger} = \Pi_{\text{null}(U_k^{(i)} \rho_k^{(ij)} U_k^{(i)\dagger})}, \quad (28)$$

we obtain the absolute irreversibility for a stochastic feedback control,

$$\overline{\lambda_{\text{fb}}} = \sum_{i \neq j, l \neq m} \frac{1}{N_{\text{copy}}^2} \sum_{k,q=0,1} p_k^{(ij)} p_q^{(lm)} \text{Tr} \left[\Pi_{\text{null}(\rho_{\text{fin},k}^{(ij)})} \rho_{\text{fin},q}^{(lm)} \right]. \quad (29)$$

$\rho_{\text{fin},k}^{(ij)} = U_k^{(i)} \rho_k^{(ij)} U_k^{(i)\dagger}$ is the feedback-operated state given that the selected particles were i and j , and measurement outcome was k .

Equation (29) shows that the absolute irreversibility $\overline{\lambda_{\text{fb}}}$ is related to how much the feedback-operated states are different for distinct selection. The term $\text{Tr}[\Pi_{\text{null}(\rho_{\text{fin},k}^{(ij)})} \rho_{\text{fin},q}^{(lm)}]$ quantifies how much the result of two

different feedback controls are different; it is 1 when the support of the two feedback-operated states are orthogonal, and 0 when identical.

We also find that the absolute irreversibility for a pure state ρ is determined by how much the state decoheres by the stochastic feedback control,

$$\overline{\lambda}_{\text{fb}} = 1 - \text{Tr} [C(\rho)^2]. \tag{30}$$

This is proved as follows. From equation (29), we use $\Pi_{\text{null}(\rho_{\text{fin},k}^{(ij)})} = 1 - \Pi_{\text{sup}(\rho_{\text{fin},k}^{(ij)})}$, where $\Pi_{\text{sup}(\rho_{\text{fin},k}^{(ij)})}$ is the projection operator onto the support of $\rho_{\text{fin},k}^{(ij)}$. As ρ is a pure state, $\rho_{\text{fin},k}^{(ij)}$ is also a pure state, and we simplify $\Pi_{\text{sup}(\rho_{\text{fin},k}^{(ij)})} = \rho_{\text{fin},k}^{(ij)}$. Then, after summing k, q and using that $\sum_k p_k^{(ij)} \rho_{\text{fin},k}^{(ij)} = C_{i \leftarrow j}(\rho)$, $\sum_q p_q^{(lm)} \rho_{\text{fin},q}^{(lm)} = C_{l \leftarrow m}(\rho)$, we obtain

$$\overline{\lambda}_{\text{fb}} = \frac{1}{N_{\text{copy}}^2} \sum_{i \neq j, l \neq m} [1 - \text{Tr} (C_{i \leftarrow j}(\rho) C_{l \leftarrow m}(\rho))], \tag{31}$$

$$= 1 - \text{Tr} \left[\frac{1}{N_{\text{copy}}^2} \sum_{i \neq j, l \neq m} C_{i \leftarrow j}(\rho) C_{l \leftarrow m}(\rho) \right]. \tag{32}$$

This is equivalent to equation (30) after summing over i, j, l, m and using equation (25).

3.3. Competition between \overline{I}_{QC} and $\overline{\lambda}_{\text{fb}}$

The result of the quantum voter model can be understood in terms of the competition between \overline{I}_{QC} and $\overline{\lambda}_{\text{fb}}$. Figures 4(a) and (b) show the entropy production rate (i.e. the negative value of the reduction rate), in the absence of bit-flip noises and a symmetric initial state, the situation of figure 2. Around the initial time, it is $\overline{\lambda}_{\text{fb}} > 0$ because different choices of copy pairs result in different feedback-operated states. For example, at the initial time, $C_{1 \leftarrow 2}(\rho) = |\Phi_+\rangle \otimes |++\rangle$ is different from $C_{4 \leftarrow 5}(\rho) = |++\rangle \otimes |\Phi_+\rangle$, as their overlap is 1/4, where

$$|\pm\rangle \equiv |0\rangle \pm |1\rangle, \tag{33}$$

$$|\Phi_+\rangle \equiv |00\rangle + |11\rangle = |++\rangle + |--\rangle, \tag{34}$$

$|\Phi_+\rangle$ being the maximally entangled two-qubit state. It can be proved (see appendix G for the derivation) that for the symmetric state one finds $\overline{\lambda}_{\text{fb}} = 3/4 \times [1 - 2/N_{\text{copy}}]$, taking the value $\overline{\lambda}_{\text{fb}} = 0$ at $N = 2$ and monotonically increasing up to 3/4 as N increases. Meanwhile, initially $\overline{I}_{\text{QC}} = 0$ because for any $C_{i \leftarrow j}$ there is no decrease of entropy when the measurement outcomes are known; $S(\rho) = 0$ and $S(\rho_k^{(ij)}) = 0$ as the initial state ρ is a pure state. Therefore, the absolute irreversibility dominates over the quantum–classical mutual information and the entropy increases by the copy processes. In addition, the purity decreases [see figure 2(b)] due to the non-vanishing $\overline{\lambda}_{\text{fb}}$, as predicted by equation (30). As time increases, the system gets closer to the consensus state [see figure 2(a)]. Then, most copy processes $C_{i \leftarrow j}$ do not change the state, hence $\overline{\lambda}_{\text{fb}} \rightarrow 0$. When $\overline{\lambda}_{\text{fb}} < \overline{I}_{\text{QC}}$, the entropy is reduced by the copy processes.

Figures 4(c) and (d) show the entropy production rate in the presence of bit-flip noise and a GHZ initial state, the situation of figure 3. In this case, the initial state yields $\overline{\lambda}_{\text{fb}} = 0$, as the state is in the perfect consensus and $\overline{I}_{\text{QC}} = 0$, as the initial state is a pure state. As time increases, the noises induce lack of consensus and decoherence. Therefore both $\overline{\lambda}_{\text{fb}}$ and \overline{I}_{QC} increase. In this case, $\overline{I}_{\text{QC}} > \overline{\lambda}_{\text{fb}}$ at all times and the entropy is always reduced by the copy processes. Note that the inequality equation (20) is always satisfied. When ignoring the absolute irreversibility $\overline{\lambda}_{\text{fb}}$, the lower bound determined by the quantum–classical mutual information predicts the entropy reduction in a too much optimistic way; see the green dashed curve in figure 4(a).

3.4. Example of the work extraction by the entangling Maxwell demon

Finally, we provide a simple example showing that the entangling Maxwell demon can indeed convert heat from the thermal bath to work using the information \overline{I}_{QC} . The work is done on an external object through the field operating the controlled-NOT operations. For example, if the NOT operations are realized by emitting or absorbing a photon, the work is extracted when the qubit emits a photon which can then provide power to another physical unit [11].

Consider two qubits interacting by a Hamiltonian

$$H = -JZ_1 \otimes Z_2, \tag{35}$$

and weakly coupled to a bath of temperature T which induces the bit-flip noise. Here Z_i is the Pauli matrix measuring the spin of qubit i in the z -direction, and $J(> 0)$ is the interaction strength between the two qubits. The bit-flip noise can be realized when (a) each qubit observable X_i is weakly coupled to the bosonic bath [38], and (b) the interaction between the qubits is weak $J \ll \hbar\Gamma_{\text{flip}}$ [4]. Note that the second condition is necessary to ensure that the bath induces independent local dissipations for each qubit. The time evolution of the qubits is governed by equation (8) with additional term $-(i/\hbar)[H, \rho]$,

$$\dot{\rho} = -\frac{i}{\hbar}[H, \rho] + \Gamma_{\text{copy}} \sum_{i \neq j} (C_{i-j}(\rho) - \rho) + \Gamma_{\text{flip}} \sum_i (X_i \rho X_i - \rho). \quad (36)$$

Once the two qubits are driven into the steady state near the maximally-entangled consensus state

$$\rho_C \equiv \frac{1}{2} (|00\rangle + |11\rangle) (\langle 00| + \langle 11|), \quad (37)$$

by the fast copy processes, they convert heat absorbed from the bath to work; the flip noise accompanies a heat absorption of $2J$ and the copy process extracts work of the same amount $2J$ into driving field which operates the measurement and feedback operation (i.e. three controlled-NOT gates) [11].

Now, we calculate the work extraction rate $\dot{W}_{\text{ext}} \equiv -\dot{W}$ for the steady state ρ_{st} formed near the maximally entangled state. The work extraction rate is equal to the heat absorption rate due to the first law of thermodynamics,

$$\dot{W}_{\text{ext}} = \Gamma_{\text{flip}} \sum_i [\text{Tr}(X_i \rho_{\text{st}} X_i H) - \text{Tr}(\rho_{\text{st}} H)]. \quad (38)$$

We find that the steady state of equation (36) satisfies

$$\rho_{\text{st}} = (1 - \epsilon)\rho_C + \epsilon\rho_{\text{FC}}, \quad (39)$$

$$\rho_{\text{FC}} = \frac{1}{2} (|01\rangle + |10\rangle) (\langle 01| + \langle 10|), \quad (40)$$

$$\epsilon = \frac{\Gamma_{\text{flip}}}{\Gamma_{\text{copy}} + 2\Gamma_{\text{flip}}}, \quad (41)$$

where ρ_{FC} is one-bit-flipped ρ_C , see appendix H for the derivation. After simple algebra using equation (82), $\text{Tr}(\rho_C H) = -J$, and $\text{Tr}(\rho_{\text{FC}} H) = J$, we obtain the work extraction rate

$$\dot{W}_{\text{ext}} = 2J\Gamma_{\text{flip}}(1 - 2\epsilon). \quad (42)$$

We compare the work extraction rate, equation (42), with the upper bound $\dot{W}_{\text{ext, ub}} = 2kT\Gamma_{\text{copy}}(\overline{I_{\text{QC}}} - \overline{\lambda_{\text{fb}}})$ dictated by the second law, equation (24). The information gain $\overline{I_{\text{QC}}} = -\epsilon \ln \epsilon - (1 - \epsilon) \ln(1 - \epsilon) \equiv h(\epsilon)$ is the binary Shannon entropy in nats, because the initial state ρ_{st} has an entropy equal to $h(\epsilon)$ and the post-measurement states are pure states with vanishing entropy. The absolute irreversibility $\overline{\lambda_{\text{fb}}}$ vanishes according to equation (29); the feedback-operated states $\rho_{\text{fin},k}^{(ij)}$ are all equal to ρ_C and

$\text{Tr} \left[\prod_{\text{null}(\rho_{\text{fin},k}^{(ij)})} \rho_{\text{fin},q}^{(lm)} \right] = 0$ for any $i \neq j$ and $k, q \in [0, 1]$. Therefore, we obtain the upper bound dictated by the second law,

$$\dot{W}_{\text{ext, ub}} = 2kT\Gamma_{\text{copy}}h(\epsilon). \quad (43)$$

The second law, $\dot{W}_{\text{ext}} \leq \dot{W}_{\text{ext, ub}}$, is verified when examining the prerequisites of the above results. Using $\Gamma_{\text{flip}}/\Gamma_{\text{copy}} = \epsilon/(1 - 2\epsilon)$, the relevant ratio becomes

$$\frac{\dot{W}_{\text{ext}}}{\dot{W}_{\text{ext, ub}}} = \frac{J}{kT} \frac{\epsilon}{h(\epsilon)}. \quad (44)$$

The factor $\epsilon/h(\epsilon)$ is smaller than 1 in the allowed range of $\epsilon \in [0, 0.5]$. We examine the other factor by further factorizing, $J/kT = (J/\hbar\Gamma_{\text{flip}})(\hbar\Gamma_{\text{flip}}/kT)$. The first factor $J/\hbar\Gamma_{\text{flip}}$ is much smaller than 1 due to the condition that the bath induces the independent local dissipations. The second factor $\hbar\Gamma_{\text{flip}}/kT$ is also much smaller than 1 as $\hbar\Gamma_{\text{flip}} = \mathcal{O}[\lim_{\omega \rightarrow 0} G(\omega)(n_{\text{B}}(\omega) + 1)] = G'(0)kT$ [38], where $G(\omega)$ is the spectral coupling density characterizing the qubit-bath coupling and $G'(0) \ll 1$ due to the weak coupling condition.

4. Conclusion

We have introduced a generic class of Maxwell demon which generates and stabilizes a many-body entanglement in the working substance. To understand the quantum dynamics, we introduced a quantum

version of the classical noisy voter model used in the context of opinion dynamics. As a result, the GHZ entanglement in the working substance was generated and stabilized against the bit-flip noises. A non-monotonic behavior of the time-evolution of the purity and entropy could be understood in terms of a competition between the information gain and the absolute irreversibility of the feedback control. We discussed how the quantum voter model can be realized in the semiconductor quantum dots and AC voltage-driven gates.

We have also formulated the second law of thermodynamics under the presence of the entangling Maxwell demon. We have obtained that upper bounds of the entropy reduction and the work extraction rates are determined by the competition between the information gain and the absolute irreversibility of the feedback control. Our finding for the upper bound for the entropy reduction rate will be helpful for stabilizing a many-body entangled state. The upper bound for the work extraction will be valuable for the exploration of the quantum information engine whose working substance is in a many-body entangled state. In these directions, our study suggests that an entangling demon is successful only when the information gain is larger than the absolute irreversibility.

As a final remark, we compare our GHZ-entanglement stabilization protocol based on the two-particle dissipations to others in the steady-state engineering. In the quantum optics community, another type of steady-state engineering based on irreversible population transfer through optical pumping is studied in the trapped ions and Rydberg atom setups [6, 21, 34, 45, 47], optionally aided by continuous feedback control [12, 25, 39]. In comparison to this, our protocol has the merit of being broadly applicable to any quantum system (not necessarily trapped ions or Rydberg atom setup) with the only requirement of the possibility of a controlled-NOT gate operation, a most basic operation implementable in diverse experimental setups. On the other hand, continuous error corrections [1, 30, 37] also have been proposed to stabilize an arbitrary state against decoherence. In comparison to this, our protocol can be more useful in a system where the number of qubits is limited, as it only requires one additional ancilla qubit for the quantum feedback control.

Acknowledgments

We thank Gonzalo Manzano, Roberta Zambrini, and Gian Luca Giorgi for useful discussions and comments. We acknowledge support from projects PACSS RTI2018-093732-B-C21, QuTTNAQMa PID2020-117347GB-I00, and the Maria de Maeztu Program for Centers and Units of Excellence in R & D, Grant MDM-2017-0711 funded by MCIN/AEI/10.13039/501100011033 and by EU through FEDER funds. Support from GOIB project MACTOPE PDR2020-12 is acknowledged. SR also acknowledges partial support from National Research Foundation of Korea (Grant No. 2021R1A6A3A03040076).

Data availability statement

The data that support the findings of this study are available upon reasonable request from the authors.

Appendix A. Nearest-neighbor connectivity in the quantum voter model

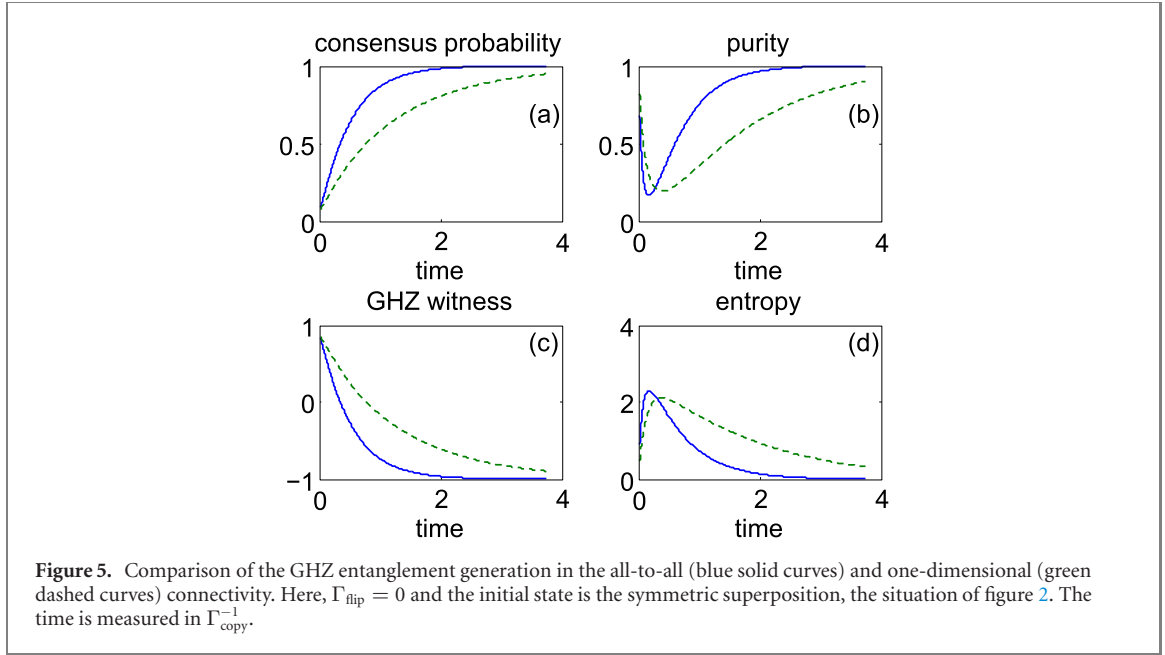
Here we present how the entanglement generation in the quantum voter model changes when the copy pair selection occurs in the one-dimensional nearest-neighbor connectivity instead of the all-to-all scenario considered in the main text. In this connectivity, a copy process $C_{i \leftrightarrow j}$ of randomly chosen pair i and j of nearest neighbor is induced with rate Γ_{copy} . We consider periodic boundary conditions, hence the allowed choices for j are $j = i \pm 1$ for $i \in [2, \dots, N-1]$, $j = 2, N$ for $i = 1$, and $j = 1, N-1$ for $i = N$.

Figure 5 shows the comparison of the GHZ entanglement generation for the two considered connectivities, in the absence of noise and the symmetric initial state, the situation of figure 2. The result shows that the all-to-all connectivity is more efficient for generating the GHZ entanglement, as the GHZ witness (c) of the all-to-all connectivity approaches to -1 faster.

Appendix B. Derivation of equation (8) and its Lindblad form

Here we show the derivation of equation (8) and that it is in the Lindblad form.

We consider the evolution of the density matrix $\rho(t)$ during a time step Δt which is smaller than $\Gamma_{\text{copy}}^{-1}$ and $\Gamma_{\text{flip}}^{-1}$ but larger than the operation time of a single copy process, i.e. the time for completing three controlled-NOT gates in figure 1(b). During the time step Δt , the copy process $C_{i \leftrightarrow j}$ occurs with probability $\Gamma_{\text{copy}} \Delta t$, the flip process X_i occurs with probability $\Gamma_{\text{flip}} \Delta t$, and the state remains the same



otherwise. Hence the time-evolved state is

$$\rho(t + \Delta t) = \Gamma_{\text{copy}} \Delta t \sum_{i \neq j} C_{i \leftarrow j}(\rho) + \Gamma_{\text{flip}} \Delta t \sum_i X_i \rho X_i + (1 - N_{\text{copy}} \Gamma_{\text{copy}} - N \Gamma_{\text{flip}}) \rho. \quad (45)$$

Dividing this equation by Δt and collecting $\dot{\rho} = \frac{\rho(t + \Delta t) - \rho(t)}{\Delta t}$, we obtain equation (8). That equation is in the Lindblad form,

$$\dot{\rho} = \Gamma_{\text{copy}} \sum_{i \neq j} \sum_{k=0,1} \left(L_k^{(ij)} \rho L_k^{(ij)\dagger} - \frac{1}{2} \{ \rho, L_k^{(ij)\dagger} L_k^{(ij)} \} \right) + \Gamma_{\text{flip}} \sum_i \left(L_i \rho L_i^\dagger - \frac{1}{2} \{ \rho, L_i^\dagger L_i \} \right), \quad (46)$$

where the Lindblad operators for the copy and flip processes are $L_k^{(ij)} = U_k^{(i)} M_k^{(ij)}$ and $L_i = X_i$, respectively. $\{ \dots, \dots \}$ is the anticommutator. This form is equivalent to equation (8) because $\sum_k L_k^{(ij)\dagger} L_k^{(ij)} = \sum_k M_k^{(ij)\dagger} U_k^{(i)\dagger} U_k^{(i)} M_k^{(ij)} = \sum_k M_k^{(ij)\dagger} M_k^{(ij)} = 1$, $L_i^\dagger L_i = X_i^2 = 1$, and

$$\sum_k \frac{1}{2} \{ \rho, L_k^{(ij)\dagger} L_k^{(ij)} \} = \frac{1}{2} \{ \rho, 1 \} = \rho, \quad (47)$$

$$\frac{1}{2} \{ \rho, L_i^\dagger L_i \} = \frac{1}{2} \{ \rho, 1 \} = \rho. \quad (48)$$

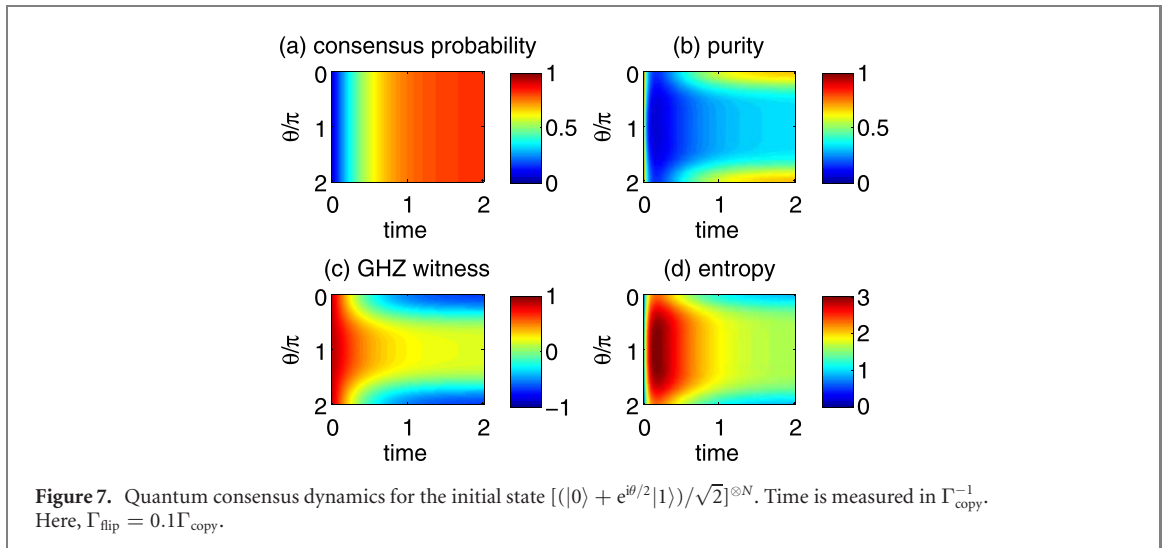
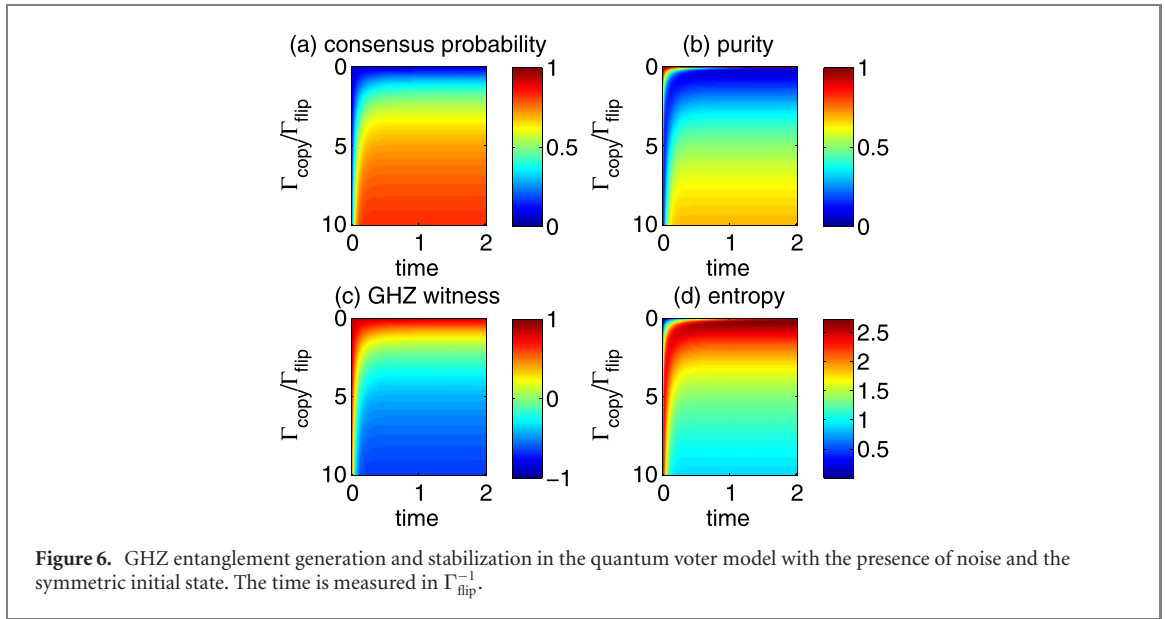
Appendix C. Quantum voter model with presence of noise and symmetric the initial state

Here, we present a supplemental result in addition to figures 2 and 3, the dynamics of the quantum voter model in the presence of bit-flip noises for the initial state of the symmetric superposition,

$$\sum_{s_1, \dots, s_N=0,1} |s_1 \dots s_N\rangle.$$

Figure 6 shows that GHZ entanglement is generated and stabilized for this case when $\Gamma_{\text{copy}} \gg \Gamma_{\text{flip}}$, namely $W_{\text{GHZ}} < -0.5$ is achieved at the stationary value when $\Gamma_{\text{copy}} > 10\Gamma_{\text{flip}}$.

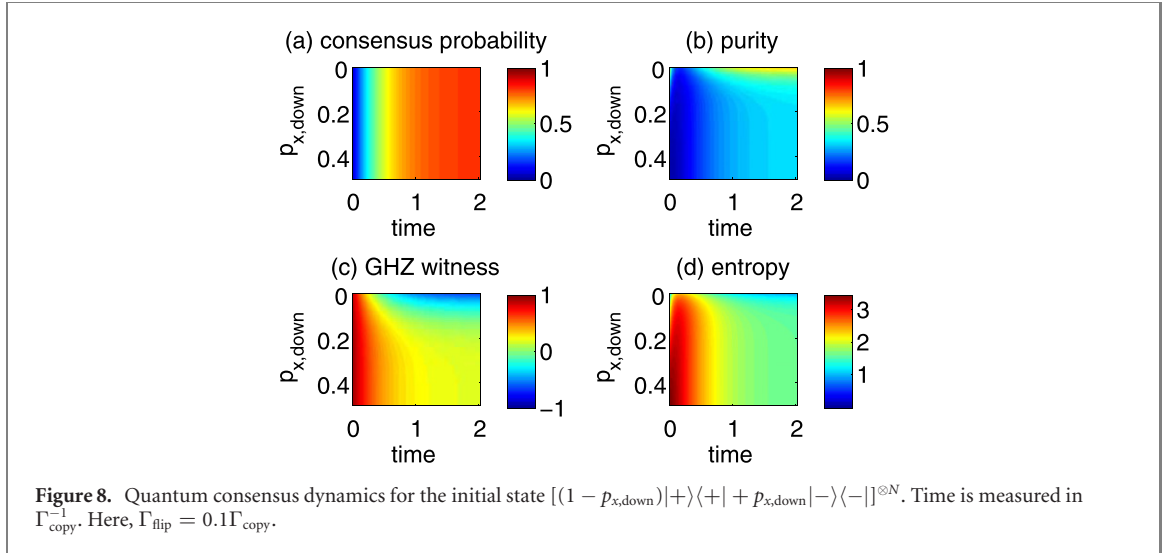
In addition, we show that GHZ entanglement is generated and stabilized even when the initial state deviates from the symmetric superposition. We consider two types of deviations which are relevant in the experimental preparation of the symmetric state using an external magnetic field in the x direction (see appendix D). First, the magnetic field can be tilted from the x direction by a azimuthal angle $\theta/2$. Then, the initial (pure) state of $[(|0\rangle + e^{i\theta/2}|1\rangle)]^{\otimes N}$ is prepared. Second, a spin can be directed toward the negative x direction due to thermal fluctuations with probability $p_{x,\text{down}} \equiv e^{-E_x/kT}$. Then, the initial (mixed) state of $[(1 - p_{x,\text{down}})|+\rangle\langle+| + p_{x,\text{down}}|-\rangle\langle-|]^{\otimes N}$ is prepared.



Figures 7 and 8 show that GHZ-entanglement is also generated even for these two types of initial states, if the deviation is sufficiently small. Figure 7 shows that $W_{\text{GHZ}} < -0.5$ is achieved at the stationary value when $\theta < 0.1\pi$. Figure 8 shows that $W_{\text{GHZ}} < -0.5$ is achieved at the stationary value when $p_{x,\text{down}} < 0.1$.

Appendix D. Experimental realization of quantum voter model

Here we discuss the experimental realization of the quantum voter model. Let us consider that the qubit states 0 and 1 are realized by the 1/2-spin up and down state in the z direction, respectively. The initial state of the symmetric superposition $\sum_{s_1, \dots, s_N=0,1} |s_1 \dots s_N\rangle = (|0\rangle + |1\rangle)^{\otimes N}$ can be prepared by applying a magnetic field in the x direction for a sufficiently large period so that the spins align to the x direction. The Zeeman splitting E_x due to the magnetic field should be much larger than the thermal energy broadening kT , as the spin is directed toward the negative x direction with probability $e^{-E_x/kT}$. After the preparation of the initial state, a quantum feedback control C_{i-k} operates in a randomly chosen qubit pair (e.g. using a random number generator), in repetitions with a frequency of Γ_{copy} . This quantum feedback control C_{i-k} can be performed experimentally, as it requires the C-NOT operation that has been recently implemented between two electron spins by resonantly driving them in an inhomogeneous Zeeman field [46]. Our system can be realized by applying the scheme to $N + 1$ quantum dots, where one quantum dot plays the role of the ancilla. The regime of the fast copy processes, $\Gamma_{\text{copy}} > \Gamma_{\text{flip}}$, can be reached in the experiments, i.e. reference [46], as $\Gamma_{\text{copy}} \sim 5$ MHz (according to the operation time ~ 200 ns of C-NOT gate) and $\Gamma_{\text{flip}} \sim 0.1$ MHz (according to the spin decoherence time of 10 μ s). As detailed in appendix C, we



find that GHZ-entanglement is also generated when the initial state deviates from the symmetric superposition, e.g. $W_{\text{GHZ}} < -0.5$ when the initial spins are tilted from the x direction by an azimuthal angle less than 0.1π , or when they are directed toward negative x direction by a probability less than 0.1.

Appendix E. Copy processes by classical feedback controls

Here we show another type of feedback control (which we called classical feedback control in the main text), which also assimilates the copy processes.

For the copy process that the qubit i copies j , the feedback controller first measures all four possible states $(s_i, s_j) = (0, 0), (0, 1), (1, 0), (1, 1)$ of the qubits. Let the measurement outcomes be $k = 0, 1, 2, 3$, respectively. The measurements are described by the projection operators $\tilde{M}_0^{(ij)} = |00\rangle\langle 00|$, $\tilde{M}_1^{(ij)} = |01\rangle\langle 01|$, $\tilde{M}_2^{(ij)} = |10\rangle\langle 10|$, and $\tilde{M}_3^{(ij)} = |11\rangle\langle 11|$. Then, according to the measurement outcome, the feedback operations $\tilde{U}_0^{(i)} = 1$, $\tilde{U}_1^{(i)} = X_i$, $\tilde{U}_2^{(i)} = X_i$, and $\tilde{U}_3^{(i)} = 1$ occur. The copy process maps the qubits from ρ to $\tilde{C}_{i \leftarrow j}(\rho)$

$$\tilde{C}_{i \leftarrow j}(\rho) = \sum_{k=0,\dots,3} \tilde{U}_k^{(i)} \tilde{M}_k^{(ij)} \rho \tilde{M}_k^{(ij)} \left(\tilde{U}_k^{(i)} \right)^\dagger. \quad (49)$$

Figure 9 shows the consensus dynamics by $\tilde{C}_{i \leftarrow j}$ in the absence of noise and the initial state of the symmetric superposition, situation of figure 2. Although the consensus probability reaches the value 1, the GHZ entanglement is not generated as $W_{\text{GHZ}} \rightarrow 0$. This is because the state approaches the classical ensemble $|00\rangle\langle 00| + |11\rangle\langle 11|$, as evidenced by the consensus probability of 1 and purity of 0.5. The decoherence appears as the measurements of the feedback control $\tilde{C}_{i \leftarrow j}$ destroy the coherence of the qubits i and j in the opinion basis $\{|0_i 0_j\rangle, |0_i 1_j\rangle, |1_i 0_j\rangle, |1_i 1_j\rangle\}$.

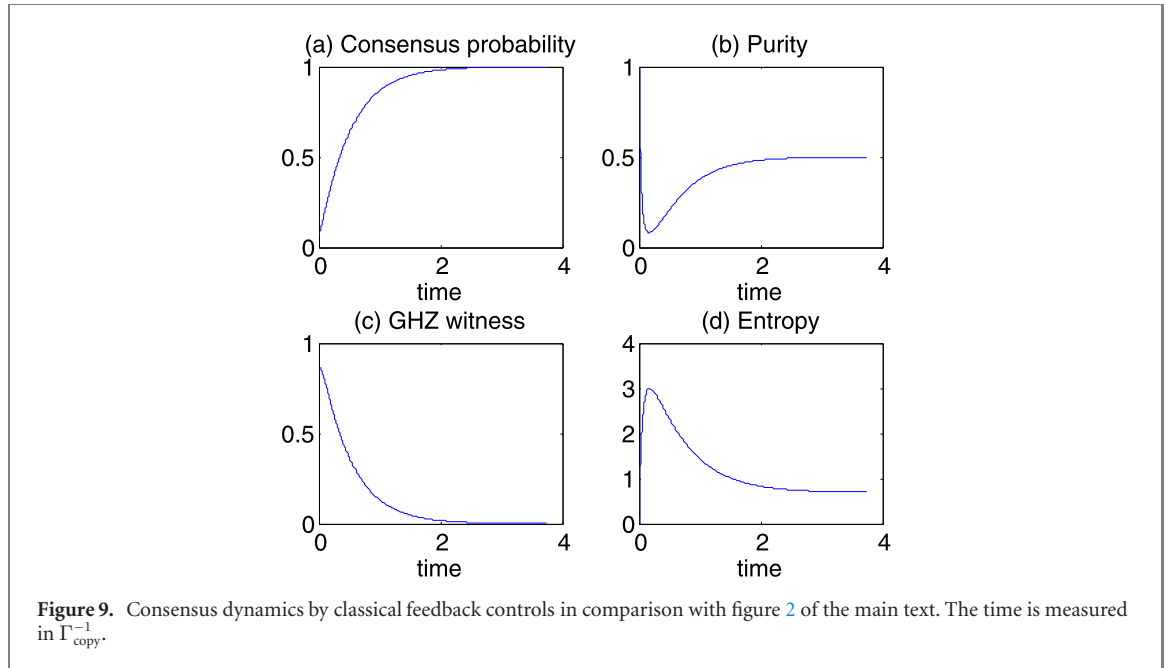
Appendix F. Upper bound of the entropy reduction rate

Here we derive the upper bound of the entropy reduction rate by the entangling Maxwell demon, $-\dot{S}_{\text{copy}}$. To this purpose, we first formulate the integral quantum fluctuation theorem (IQFT) for the entropy change, see equation (69). The formulation is based on the approach of reference [13] on the IQFT for a single quantum feedback control. Then, by applying Jensen's inequality to the obtained IQFT, we derive the upper bound for the entropy reduction rate, equation (20). The notations in the derivations are presented in the case of the quantum voter model, but they are straightforwardly generalized for a generic entangling Maxwell demon.

To obtain the IQFT, let us consider a thought experiment monitoring the time evolution during a small time Δt which is much smaller than the repetition period $\Gamma_{\text{copy}}^{-1}$ but larger than the operation time of a feedback control (i.e. the time for completing three C-NOT gates in the case of the quantum voter model).

- The initial state ρ is measured in the basis $\{|x\rangle\}$ which diagonalizes ρ .
- We monitor, if any, which particles were selected for a quantum feedback control.

If a pair of qubits i and j are selected,



- (c) We monitor the measurement outcome k (which is 0 when $s_i = s_j$ and 1 otherwise) of the feedback control applied to the selected qubits.
- (d) We measure the post-measurement state in the basis $\{|y\rangle\}$ which diagonalizes $\rho_k^{(ij)}$ defined by equation (6).
- (e) We measure the feedback-operated state in the basis $\{|z\rangle\}$ that diagonalizes a reference state ρ_r [13].

A quantum transition is described by the record of all measurements (x, ij, k, y, z) . The corresponding transition probability $P(x, ij, k, y, z)$ is the product of the probabilities of each monitoring (a)–(e),

$$P(x, ij, k, y, z) = p_a(x)p_{\text{copy}}p_c(k|x, ij)p_d(y|x, ij, k)p_e(z|ij, k, y) + \mathcal{O}(\Gamma_{\text{copy}}\Delta t)^2, \quad (50)$$

$$p_a(x) = \langle x|\rho|x\rangle, \quad (51)$$

$$p_{\text{copy}} = \Gamma_{\text{copy}}\Delta t, \quad (52)$$

$$p_c(k|x, ij) = |\langle x|M_k^{(ij)}|x\rangle|^2, \quad (53)$$

$$p_d(y|x, ij, k) = |\langle y|M_k^{(ij)}|x\rangle|^2/p_c(k|x, ij), \quad (54)$$

$$p_e(z|ij, k, y) = |\langle z|U_k^{(i)}|y\rangle|^2. \quad (55)$$

The transition probability P is related to the probability $P^{(ij)}$ given that the particles i and j are selected,

$$P(x, ij, k, y, z) = p_{\text{copy}}P^{(ij)}(x, k, y, z) + \mathcal{O}(\Gamma_{\text{copy}}\Delta t)^2, \quad (56)$$

$$P^{(ij)}(x, k, y, z) = p_a(x)p_c(k|x, ij)p_d(y|x, ij, k)p_e(z|ij, k, y). \quad (57)$$

Following the approach of reference [13], we define the unaveraged entropy change σ by the feedback controls and unaveraged quantum–classical mutual information i_{QC} [13] for a transition (x, ij, k, y, z) ,

$$\sigma(x, z) = \ln p_a(x) - \ln p_r(z), \quad (58)$$

$$i_{\text{QC}}(x, ij, k, y) = -\ln p_a(x) + \ln p(y|ij, k). \quad (59)$$

Here $p_r(z) \equiv \langle z|\rho_r|z\rangle$ is the probability distribution of the reference state, and $p(y|ij, k) = \langle y|\rho_k^{(ij)}|y\rangle$ is the probability distribution of the post-measurement state $\rho_k^{(ij)}$. If no feedback control has occurred, $\sigma = 0$ and $i_{\text{QC}} = 0$ because we want to describe entropy reduction by the feedback controls.

The expectation value of σ provides an lower-bound for the entropy change by the feedback controls, \dot{S}_{copy} [see equation (18)], during the time Δt

$$\langle \sigma \rangle = N_{\text{copy}} \Gamma_{\text{copy}} \{S(C(\rho)) - S(\rho)\} \Delta t, \tag{60}$$

$$\leq \dot{S}_{\text{copy}} \Delta t, \tag{61}$$

when choosing the reference state as the result of the stochastic feedback control without knowing which particles were selected,

$$\rho_r = C(\rho). \tag{62}$$

Equation (60) is derived by relating $\langle \sigma \rangle$ to a expectation value $\langle \sigma \rangle^{(ij)}$ given that the particles i and j were selected, and using that $\langle \sigma \rangle^{(ij)} = -S(\rho) - \text{Tr}[C_{i \leftarrow j}(\rho) \ln C(\rho)]$ (see reference [13]).

$$\begin{aligned} \langle \sigma \rangle &= \sum_{i \neq j} p_{\text{copy}} \langle \sigma \rangle^{(ij)} \\ &= \sum_{i \neq j} p_{\text{copy}} [-S(\rho) - \text{Tr}[C_{i \leftarrow j}(\rho) \ln C(\rho)]] \\ &= -N_{\text{copy}} p_{\text{copy}} S(\rho) - N_{\text{copy}} p_{\text{copy}} \text{Tr}[C(\rho) \ln C(\rho)] \\ &= N_{\text{copy}} p_{\text{copy}} [-S(\rho) + S(C(\rho))] \\ &= N_{\text{copy}} \Gamma_{\text{copy}} [-S(\rho) + S(C(\rho))] \Delta t. \end{aligned} \tag{63}$$

Equation (61) is derived when applying the concavity of the von Neumann entropy to the definition of \dot{S}_{copy} ,

$$\dot{S}_{\text{copy}} = \frac{S(N_{\text{copy}} p_{\text{copy}} C(\rho) + (1 - N_{\text{copy}} p_{\text{copy}}) \rho) - S(\rho)}{\Delta t}. \tag{64}$$

The expectation value of i_{QC} is the average quantum–classical mutual information obtained in the feedback controls during the time Δt ,

$$\langle i_{\text{QC}} \rangle = \sum_{i \neq j} p_{\text{copy}} I_{\text{QC}}^{(ij)}, \tag{65}$$

$$= N_{\text{copy}} \Gamma_{\text{copy}} \overline{I_{\text{QC}}} \Delta t. \tag{66}$$

To obtain the IQFT, we express $\langle e^{-\sigma - i_{\text{QC}}} \rangle$ by an expectation value $\langle e^{-\sigma - i_{\text{QC}}} \rangle^{(ij)}$ given that the particles i and j were selected. We use the integral fluctuation theorem for a single feedback control [13],

$$\langle e^{-\sigma - i_{\text{QC}}} \rangle^{(ij)} = 1 - \lambda_{\text{fb}}^{(ij)}, \tag{67}$$

and use that if no feedback control has occurred, $\sigma = 0$ and $i_{\text{QC}} = 0$. Then, we obtain

$$\begin{aligned} \langle e^{-\sigma - i_{\text{QC}}} \rangle &= \sum_{i \neq j} p_{\text{copy}} \langle e^{-\sigma - i_{\text{QC}}} \rangle^{(ij)} + \left(1 - \sum_{i \neq j} p_{\text{copy}}\right) \\ &= \sum_{i \neq j} p_{\text{copy}} (1 - \lambda_{\text{fb}}^{(ij)}) + (1 - N_{\text{copy}} p_{\text{copy}}), \\ &= 1 - N_{\text{copy}} p_{\text{copy}} \overline{\lambda_{\text{fb}}}. \end{aligned} \tag{68}$$

This leads to the IQFT during the small time $\Delta t \ll \Gamma_{\text{copy}}^{-1}$ (note that equations (50) and (56) are only valid for such small time)

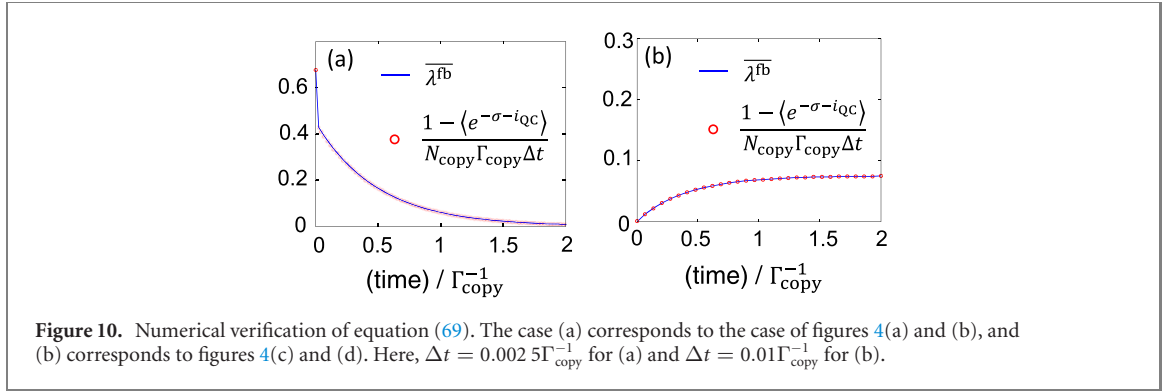
$$\langle e^{-\sigma - i_{\text{QC}}} \rangle = 1 - N_{\text{copy}} \Gamma_{\text{copy}} \overline{\lambda_{\text{fb}}} \Delta t + \mathcal{O}(\Gamma_{\text{copy}} \Delta t)^2. \tag{69}$$

Figure 10 shows that equation (69) is indeed satisfied for the situations of figure 4.

Finally, we obtain the upper bound of the entropy reduction rate $-\dot{S}_{\text{copy}}$ by applying Jensen’s inequality, $e^{\langle X \rangle} \leq \langle e^X \rangle$, to equation (69) and taking the limit of $\Gamma_{\text{copy}} \Delta t \rightarrow 0$,

$$\begin{aligned} \dot{S}_{\text{copy}} &\geq \frac{\langle \sigma \rangle}{\Delta t} \\ &\geq \frac{1}{\Delta t} [-\langle i_{\text{QC}} \rangle - \ln [1 - N_{\text{copy}} \Gamma_{\text{copy}} \overline{\lambda_{\text{fb}}} \Delta t]] \\ &= N_{\text{copy}} \Gamma_{\text{copy}} [-\overline{I_{\text{QC}}} + \overline{\lambda_{\text{fb}}}] . \end{aligned} \tag{70}$$

In the last equality, we have used equation (66) and that $\Gamma_{\text{copy}} \Delta t$ is small.



Appendix G. Absolute irreversibility in the quantum voter model for the symmetric initial state

Here we derive that the absolute irreversibility $\overline{\lambda}_{\text{fb}}$ in the quantum voter model for the symmetric initial state $\rho = (\sum_{s_1, \dots, s_N=0,1} |s_1 \dots s_N\rangle / \sqrt{2^N})$ (h.c.)

$$\overline{\lambda}_{\text{fb}} = \frac{3}{4} \left[1 - \frac{2}{N(N-1)} \right]. \quad (71)$$

We use equation (31). We evaluate the overlap $\text{Tr}[C_{i \leftarrow j}(\rho)C_{k \leftarrow m}(\rho)]$ by dividing the choices of i, j, l and m in three cases.

- When the qubit pair (i, j) does not share any common qubit with the pair (l, m) , the overlap $\text{Tr}[C_{i \leftarrow j}(\rho)C_{k \leftarrow m}(\rho)]$ is $1/4$. This is because the overlap is the same as $\text{Tr}[C_{1 \leftarrow 2}(\rho)C_{N-1 \leftarrow N}(\rho)]$ due to the permutation symmetry of qubits, and it equals $|\langle \Phi_+ + \dots + | + \dots + \Phi_+ \rangle|^2 = |\langle \Phi_+ + + | + + \Phi_+ \rangle|^2 = 1/4$.
- When the qubit pair (i, j) shares one common qubit with the pair (l, m) , the overlap $\text{Tr}[C_{i \leftarrow j}(\rho)C_{k \leftarrow m}(\rho)]$ is also $1/4$. This is because the overlap equals $\text{Tr}[C_{1 \leftarrow 2}(\rho)C_{2 \leftarrow 3}(\rho)]$ due to the permutation symmetry, and it equals $|\langle \Phi_+ + \dots + | + \Phi_+ + \dots + + \rangle|^2 = |\langle \Phi_+ + | + \Phi_+ \rangle|^2 = 1/4$.
- When the qubit pair (i, j) shares two common qubits with the pair (l, m) , the overlap $\text{Tr}[C_{i \leftarrow j}(\rho)C_{k \leftarrow m}(\rho)]$ is 1, due to the permutation symmetry.

We count the number of the choices of i, j, l , and m in the cases (a)–(c). The total number of choices in all the cases is $[N(N-1)]^2$, due to the all-to-all network connectivity, $i \neq j$ and $l \neq m$. The number of choices in the case (c) is $2N(N-1)$. The number of choices in the cases (a) and (b) is $[N(N-1)]^2 - 2N(N-1)$. Using these in equation (31)

$$\overline{\lambda}_{\text{fb}} = \frac{[N(N-1)]^2 - 2N(N-1)}{N_{\text{copy}}^2} \left(1 - \frac{1}{4} \right) + \frac{2N(N-1)}{N_{\text{copy}}^2} (1 - 1). \quad (72)$$

Replacing $N_{\text{copy}} = N(N-1)$, this is equivalent to equation (71).

Appendix H. Steady-state solution for the two-qubit information engine

Here we derive the steady-state solution near the maximally entangled state in situation of the two-qubit information engine discussed in section 3.4. We try the following ansatz

$$\rho_{\text{st}} = (1 - \epsilon)\rho_{\text{C}} + \epsilon\rho_{\text{FC}}, \quad (73)$$

to which we apply the steady-state condition $\dot{\rho}_{\text{st}} = 0$ with the master equation equation (36). The unitary part of the Liouvillian vanishes,

$$[H, \rho_{\text{st}}] = 0. \quad (74)$$

This is a consequence of the equalities

$$Z_1 \otimes Z_2 \rho_{\text{C}} Z_1 \otimes Z_2 = \rho_{\text{C}}, \quad (75)$$

$$Z_1 \otimes Z_2 \rho_{\text{FC}} Z_1 \otimes Z_2 = \rho_{\text{FC}}, \quad (76)$$

which can be easily proved using the definitions of equations (37) and (40).

To calculate the other parts of the Liouvillian, we use

$$C_{i\leftarrow j}(\rho_C) = \rho_C, \quad (77)$$

$$C_{i\leftarrow j}(\rho_{FC}) = \rho_C, \quad (78)$$

$$X_i \rho_C X_i = \rho_{FC}, \quad (79)$$

$$X_i \rho_{FC} X_i = \rho_C, \quad (80)$$

for any i and $j \neq i$. These lead to

$$C_{i\leftarrow j}(\rho_{st}) - \rho_{st} = \epsilon(\rho_C - \rho_{FC}), \quad (81)$$

$$X_i \rho_{st} X_i - \rho_{st} = (2\epsilon - 1)(\rho_C - \rho_{FC}), \quad (82)$$

$$\dot{\rho}_{st} = (\rho_C - \rho_{FC})[2\epsilon\Gamma_{\text{copy}} + 2(2\epsilon - 1)\Gamma_{\text{flip}}]. \quad (83)$$

Therefore, the steady-state condition is satisfied when

$$\epsilon = \frac{\Gamma_{\text{flip}}}{\Gamma_{\text{copy}} + 2\Gamma_{\text{flip}}}. \quad (84)$$

ORCID iDs

Sungguen Ryu  <https://orcid.org/0000-0003-1587-9372>

Rosa López  <https://orcid.org/0000-0002-3717-6347>

Raúl Toral  <https://orcid.org/0000-0003-2046-7620>

References

- [1] Ahn C, Doherty A C and Landahl A J 2002 Continuous quantum error correction via quantum feedback control *Phys. Rev. A* **65** 042301
- [2] Belenchia A, Mancino L, Landi G T and Paternostro M 2020 Entropy production in continuously measured Gaussian quantum systems *npj Quantum Inf.* **6** 97
- [3] Castellano C, Fortunato S and Loreto V 2009 Statistical physics of social dynamics *Rev. Mod. Phys.* **81** 591–646
- [4] Cattaneo M, Giorgi G L, Maniscalco S and Zambrini R 2019 Local versus global master equation with common and separate baths: superiority of the global approach in partial secular approximation *New J. Phys.* **21** 113045
- [5] Chaves R, Brask J B, Markiewicz M, Kołodyński J and Acín A 2013 Noisy metrology beyond the standard quantum limit *Phys. Rev. Lett.* **111** 120401
- [6] Cho J, Bose S and Kim M S 2011 Optical pumping into many-body entanglement *Phys. Rev. Lett.* **106** 020504
- [7] Clifford P and Sudbury A 1973 A model for spatial conflict *Biometrika* **60** 581–8
- [8] Diehl S, Micheli A, Kantian A, Kraus B, Büchler H P and Zoller P 2008 Quantum states and phases in driven open quantum systems with cold atoms *Nat. Phys.* **4** 878–83
- [9] Dür W, Skotiniotis M, Froewis F and Kraus B 2014 Improved quantum metrology using quantum error correction *Phys. Rev. Lett.* **112** 080801
- [10] Elouard C and Jordan A N 2018 Efficient quantum measurement engines *Phys. Rev. Lett.* **120** 260601
- [11] Elouard C, Herrera-Martí D, Huard B and Auffèves A 2017 Extracting work from quantum measurement in Maxwell’s demon engines *Phys. Rev. Lett.* **118** 260603
- [12] Feng W, Wang P, Ding X, Xu L and Li X-Q 2011 Generating and stabilizing the Greenberger–Horne–Zeilinger state in circuit QED: joint measurement, Zeno effect, and feedback *Phys. Rev. A* **83** 042313
- [13] Funo K, Murashita Y and Ueda M 2015 Quantum nonequilibrium equalities with absolute irreversibility *New J. Phys.* **17** 075005
- [14] Giovannetti V, Lloyd S and Maccone L 2006 Quantum metrology *Phys. Rev. Lett.* **96** 010401
- [15] Granovsky B L and Madras N 1995 The noisy voter model *Stoch. Process. Appl.* **55** 23–43
- [16] Holley R A and Liggett T M 1975 Ergodic theorems for weakly interacting infinite systems and the voter model *Ann. Probab.* **3** 643–63
- [17] Kim S W, Sagawa T, De Liberato S and Ueda M 2011 Quantum Szilard engine *Phys. Rev. Lett.* **106** 070401
- [18] Koski J V, Maisi V F, Sagawa T and Pekola J P 2014 Experimental observation of the role of mutual information in the nonequilibrium dynamics of a Maxwell demon *Phys. Rev. Lett.* **113** 030601
- [19] Koski J V, Kutvonen A, Khaymovich I M, Ala-Nissila T and Pekola J P P 2015 On-chip Maxwell’s demon as an information-powered refrigerator *Phys. Rev. Lett.* **115** 260602
- [20] Leibfried D et al 2005 Creation of a six-atom ‘Schrödinger cat’ state *Nature* **438** 639–42
- [21] Lin Y, Gaebler J P, Reiter F, Tan T R, Bowler R, Sørensen A S, Leibfried D and Wineland D J 2013 Dissipative production of a maximally entangled steady state of two quantum bits *Nature* **504** 415–8
- [22] Liuzzo-Scorpo P, Correa L, Schmidt R and Adesso G 2016 Thermodynamics of quantum feedback cooling *Entropy* **18** 48
- [23] Manzano G, Subero D, Maillet O, Fazio R, Pekola J P and Roldán É 2021 Thermodynamics of gambling demons *Phys. Rev. Lett.* **126** 080603

- [24] Monz T *et al* 2011 14-qubit entanglement: creation and coherence *Phys. Rev. Lett.* **106** 130506
- [25] Morigi G, Eschner J, Cormick C, Lin Y, Leibfried D and Wineland D J 2015 Dissipative quantum control of a spin chain *Phys. Rev. Lett.* **115** 200502
- [26] Murashita Y and Ueda M 2017 Gibbs paradox revisited from the fluctuation theorem with absolute irreversibility *Phys. Rev. Lett.* **118** 060601
- [27] Murashita Y, Funo K and Ueda M 2014 Nonequilibrium equalities in absolutely irreversible processes *Phys. Rev. E* **90** 042110
- [28] Nielsen M A and Chuang I L 2010 *Quantum Computation and Quantum Information* (Cambridge: Cambridge University Press)
- [29] Parrondo J M R, Horowitz J M and Sagawa T 2015 Thermodynamics of information *Nat. Phys.* **11** 131–9
- [30] Paz J P and Zurek W H 1998 Continuous error correction *Proc. R. Soc. A* **454** 355–64
- [31] Pekola J P P 2015 Towards quantum thermodynamics in electronic circuits *Nat. Phys.* **11** 118–23
- [32] Peralta A F, Carro A, Miguel M S and Toral R 2018 Stochastic pair approximation treatment of the noisy voter model *New J. Phys.* **20** 103045
- [33] Ptaszyński K and Esposito M 2019 Thermodynamics of quantum information flows *Phys. Rev. Lett.* **122** 150603
- [34] Reiter F, Reeb D and Sørensen A S 2016 Scalable dissipative preparation of many-body entanglement *Phys. Rev. Lett.* **117** 040501
- [35] Ribezzi-Crivellari M and Ritort F 2019 Large work extraction and the Landauer limit in a continuous Maxwell demon *Nat. Phys.* **15** 660–4
- [36] Sagawa T and Ueda M 2008 Second law of thermodynamics with discrete quantum feedback control *Phys. Rev. Lett.* **100** 080403
- [37] Sarovar M, Ahn C, Jacobs K and Milburn G J 2004 Practical scheme for error control using feedback *Phys. Rev. A* **69** 052324
- [38] Schaller G 2014 *Open Quantum Systems Far from Equilibrium* vol 881 (Berlin: Springer)
- [39] Stevenson R N, Hope J J and Carvalho A R R 2011 Engineering steady states using jump-based feedback for multipartite entanglement generation *Phys. Rev. A* **84** 022332
- [40] Ticozzi F and Viola L 2012 Stabilizing entangled states with quasi-local quantum dynamical semigroups *Phil. Trans. R. Soc. A* **370** 5259–69
- [41] Ticozzi F and Viola L 2014 Steady-state entanglement by engineered quasi-local Markovian dissipation *Quantum Inf. Comput.* **14** 265–94
- [42] Verstraete F, Wolf M M and Cirac I J 2009 Quantum computation and quantum-state engineering driven by dissipation *Nat. Phys.* **5** 633–6
- [43] Wasilewski W, Jensen K, Krauter H, Renema J J, Balabas M V and Polzik E S 2010 Quantum noise limited and entanglement-assisted magnetometry *Phys. Rev. Lett.* **104** 133601
- [44] Wintermantel T M, Wang Y, Lochead G, Shevate S, Brennen G K and Whitlock S 2020 Unitary and nonunitary quantum cellular automata with Rydberg arrays *Phys. Rev. Lett.* **124** 070503
- [45] Wiseman H M and Milburn G J 2009 *Quantum Measurement and Control* (Cambridge: Cambridge University Press)
- [46] Zajac D M, Sigillito A J, Russ M, Borjans F, Taylor J M, Burkard G and Petta J R R 2018 Resonantly driven CNOT gate for electron spins *Science* **359** 439–42
- [47] Zhang J, Liu Y-x, Wu R-B, Jacobs K and Nori F 2017 Quantum feedback: theory, experiments, and applications *Phys. Rep.* **679** 1–60